Int. J. Heat Mass Transfer. Vol. 7, pp. 875–890. Pergamon Press 1964. Printed in Great Britain

HEAT TRANSFER THROUGH THE TURBULENT INCOMPRESSIBLE BOUNDARY LAYER ON A FLAT PLATE

A. P. HATTON
Manchester College of Science and Technology, Manchester 1

(*Received* 26 *November* 1963 *and in revised form* 1 *February* 1964)

Abstract—From the assumption that the dimensionless velocity profile in a turbulent incompressible boundary layer obeys the well-known universal profile it is shown that the boundary layer thickness, and the shear stress and eddy diffusivity variations through the thickness at any Reynolds number, may be derived. The resulting variations, expressed in dimensionless form, are shown to be only weakly dependent on Reynolds number.

Using the additional assumption that the eddy diffusivities for momentum and heat are equal the energy equation is solved numerically to obtain the Stanton number variation with Reynolds number for several Prandtl numbers. Results are given for Prandtl numbers of 0·01, 0·1, 0·7, 1·0 and 10 for a number of different positions of a step temperature distribution on the flat plate.

NOMENCLATURE

- C, temperature parameter defined by equation (21);
- C_f, local coefficient of friction;
- C_i, constant as defined by equation (20);
- C_p, specific heat at constant pressure;
- h, local heat-transfer coefficient;
- k, thermal conductivity;
- l, unheated starting length;
- n, constant in Deissler profile;
- Pr, Prandtl number $= C\mu/k$;
- R, Reynolds number $= u_s x/\nu$;
- R_l, Reynolds number at distance l;
- R_x, Reynolds number at distance x;
- Sp, Spalding function $(= St \, . \, Pr \, . \, u_s^+)$;
- St, Stanton number;
- t, temperature;
- t_w, temperature at the wall;
- t_s, temperature in the free stream;
- u, temporal mean velocity in the x-direction;
- u_s, free stream velocity;
- u^+, dimensionless velocity $u/\sqrt{(\tau_w/\rho)}$;
- v, temporal mean velocity in the y-direction;
- x, distance along the plate;
- x^+, dimensionless distance $= \int_l^x \frac{\sqrt{(\tau_w/\rho)}}{\nu} . \, dx$;
- y, distance normal to the wall;
- y^+, dimensionless distance normal to the wall $\frac{y\sqrt{(\tau_w/\rho)}}{\nu}$;
- y_s^+, y^+ at the edge of the velocity boundary layer where $u^+ = u_s^+$;
- α, thermal molecular diffusivity $k/\rho C_p$;
- β, $= \frac{1}{Pr} + \frac{\epsilon_h}{\nu}$;
- β', $\partial\beta/\partial y^+$;
- ΔR, step length in R;
- Δy^+, step length in y^+;
- ϵ_h, eddy diffusivity for heat;
- ϵ_m, eddy diffusivity for momentum;
- η, variable used in von Mises transformation;
- θ, dimensionless temperature $\frac{t - t_w}{t_s - t_w}$;
- ν, kinematic viscosity of fluid;
- ξ, variable used in von Mises transformation;
- ρ, fluid density;
- τ, shear stress;
- τ_w, shear stress at the wall;
- ψ, stream function.

INTRODUCTION

THIS article describes a solution to the energy equation when a fluid flows at constant velocity parallel to a flat plate under conditions when there is turbulent incompressible boundary layer. The plate is considered to be at the stream temperature for a certain distance from the leading edge and then at a different temperature over the remainder.

Owing to the limited knowledge concerning heat transport in turbulent flow near surfaces, solutions to this problem involve a high degree of empiricism. Earlier solutions or empirical correlations of experimental results were given by Rubesin [1], Scesa and Sauer [2], Owen and Ormerod [3], Furber [4], Reynolds, Kays and Kline [5] but these are all restricted to cases in which the Prandtl number is unity or near. More general solutions have appeared recently following a new approach due to Spalding [6] who also proposed a new form of the law of the wall [7] in which a single equation is used to describe the dimensionless velocity variation in the boundary layer. Kestin and Persen [8], Smith and Shah [9] and Kestin and Gardner [10] have extended Spalding's work and produced solutions to the problem for a wide range of Prandtl numbers. In these analyses however, the assumption is made that the thermal boundary layer is thin compared with the velocity boundary layer and this is justified only for certain Prandtl number ranges. If the Prandtl number be less than unity then it is possible for the temperature boundary layer to extend beyond the velocity boundary layer so that the analysis of [8, 9, 10] are restricted to $Pr \geqslant 1$.

A comprehensive survey of the state of knowledge on this problem is presented by Kestin and Richardson [11] but it appears that no solution is yet available for low Prandtl numbers and it is the object of this work to present a solution which is applicable to all values of this parameter.

MOMENTUM EQUATION

The momentum and continuity equations for an incompressible turbulent boundary layer with zero pressure gradient and with the introduction of the eddy diffusivity for momentum ϵ_m may be written

$$u\frac{\partial u}{\partial x} + v\frac{\partial u}{\partial y} = \frac{\partial}{\partial y}\left\{(\nu + \epsilon_m)\frac{\partial u}{\partial y}\right\} \tag{1}$$

$$\frac{\partial u}{\partial x} + \frac{\partial v}{\partial y} = 0 \tag{2}$$

In (1) is included the shear stress definition

$$\frac{\tau}{\rho} = (\nu + \epsilon_m)\frac{\partial u}{\partial y}$$

Following the procedure suggested by Spalding [6], the von Mises transformation is used such that

$$u = \frac{\partial \psi}{\partial y}$$

$$v = -\frac{\partial \psi}{\partial x}$$

$\xi = f(x)$ and $f(x)$ is chosen equal to x

$\eta = f(\psi)$ and $f(\psi)$ is chosen equal to ψ.

Then

$$\frac{\partial}{\partial x}[u(x, y)] = \frac{\partial}{\partial \xi}[u(\xi, \eta)]\frac{\partial \xi}{\partial x} + \frac{\partial}{\partial \eta}[u(\xi, \eta)]\frac{\partial \eta}{\partial x}$$

and similarly for the y derivative.

It is easily shown that

$$\frac{\partial u}{\partial x} = \frac{\partial u}{\partial \xi} + \frac{\partial u}{\partial \eta}\cdot\frac{\partial \eta}{\partial x}$$

$$\frac{\partial u}{\partial y} = \frac{\partial u}{\partial \eta}\cdot\frac{\partial \eta}{\partial y}$$

$$\frac{\partial \tau}{\partial y} = \frac{\partial \tau}{\partial \eta}\cdot\frac{\partial \eta}{\partial y}$$

and with

$$\xi = x, \quad \eta = \psi$$

we obtain

$$\frac{\partial u}{\partial x} = \frac{1}{\rho}\frac{\partial \tau}{\partial \psi} \tag{3}$$

We introduce the dimensionless variables u^+ and y^+ at this point and obtain

$$\frac{\partial \psi}{\partial y^+} = \nu u^+$$

We now assume, on the basis of experimental evidence, that u^+ is a function of y^+ only in a turbulent boundary layer, i.e. that there is a fixed functional relationship termed the "law of the wall". Thus we may write

$$\frac{\mathrm{d}\psi}{\mathrm{d}y^+} = \nu u^+$$

This may be substituted in (3) to give

$$\frac{\partial u}{\partial x} = \frac{1}{\nu \, . \, \rho \, . \, u^+} \cdot \frac{\partial \tau}{\partial y^+}$$

The dimensionless variable $R(=u_s x/\nu)$ is now introduced and u_s is taken constant.

Hence

$$u_s^2 \frac{\partial}{\partial R}\left(\frac{u^+}{u_s^+}\right) = \frac{1}{\rho u^+} \frac{\partial \tau}{\partial y^+}$$

Expanding this expression and remembering that $(\partial u^+/\partial R) = 0$

$$-(u^+)^2 \frac{\partial u_s^+}{\partial R} = \frac{1}{\tau_w} \frac{\partial \tau}{\partial y^+}$$

Integrating from $0 \to y^+$ gives

$$-\int_0^{y^+} (u^+)^2 \frac{\mathrm{d}u_s^+}{\mathrm{d}R} \cdot \mathrm{d}y^+ = \frac{\tau - \tau_w}{\tau_w}$$

Also $(\mathrm{d}u_s^+/\mathrm{d}R)$ is not a function of y^+ thus

$$-\frac{\mathrm{d}u_s^+}{\mathrm{d}R} \int_0^{y^+} (u^+)^2 \, \mathrm{d}y^+ = \frac{\tau}{\tau_w} - 1$$

At $\qquad y = y_s^+, \quad \tau = 0$

so that

$$\frac{\mathrm{d}u_s^+}{\mathrm{d}R} = \frac{1}{\int_0^{y_s^+} (u^+)^2 \, \mathrm{d}y^+} \tag{4}$$

and

$$\frac{\tau}{\tau_w} = 1 - \frac{\int_0^{y^+} (u^+)^2 \, \mathrm{d}y^+}{\int_0^{y_s^+} (u^+)^2 \, \mathrm{d}y^+} \tag{5}$$

Equations (4) and (5) may be used to determine the Reynolds number $-u_s^+$ relation if the law of the wall be known and the variation of shear stress at any particular value of the Reynolds number.

The eddy diffusivity for momentum variation follows from (5) since

$$\frac{\tau}{\rho} = (\nu + \epsilon_m) \frac{\partial u}{\partial y}$$

and

$$\frac{\partial u}{\partial y} = u \frac{\partial u}{\partial \psi}$$

$$= \frac{\tau_w}{\rho \nu} \cdot \frac{\mathrm{d}u^+}{\mathrm{d}y^+}$$

Thus

$$\frac{\tau}{\tau_w} = \frac{\nu + \epsilon_m}{\nu} \frac{\mathrm{d}u^+}{\mathrm{d}y^+}$$

or

$$\frac{\epsilon_m}{\nu y_s^+} = \frac{1}{y_s^+}\left(\frac{\tau}{\tau_w} \cdot \frac{\mathrm{d}y^+}{\mathrm{d}u^+} - 1\right) \tag{6}$$

Equation (6) in conjunction with (5) gives the variation of eddy diffusivity through the boundary layer for any particular value of y_s^+ (or R). This is a major step in the analysis since the assumption will be made that the eddy diffusivity for momentum is equal to that for heat.

Before proceeding to calculations involving particular forms of the "law of the wall" we re-form (4) as

$$\frac{\mathrm{d}R}{\mathrm{d}u_s^+} = \int_0^{y_s^+} (u^+)^2 \, \mathrm{d}y^+$$

or

$$R_2 - R_1 = \int_{y_{s1}^+}^{y_{s2}^+} \left[\int_0^{y_s^+} (u^+)^2 \, \mathrm{d}y^+\right] \mathrm{d}u_s^+ \tag{7}$$

LAWS OF THE WALL

A number of expressions have been proposed to fit the $u^+ - y^+$ relationship which, from experiments, appears to have a fixed shape independent of Reynolds number. These are well reviewed in [7]. In this analysis two proposed forms are used and compared, namely, that due to Deissler [12] and that due to Spalding [7].

(a) *Deissler's law*

Two separate expressions were put forward by Deissler which cover different ranges of y^+

$$0 < y^+ < 26 \quad \frac{\mathrm{d}u^+}{\mathrm{d}y^+} = \frac{1}{1 + 0{\cdot}0154\, u^+ y^+ [1 - \exp(-0{\cdot}0154\, u^+ y^+)]} \tag{8}$$

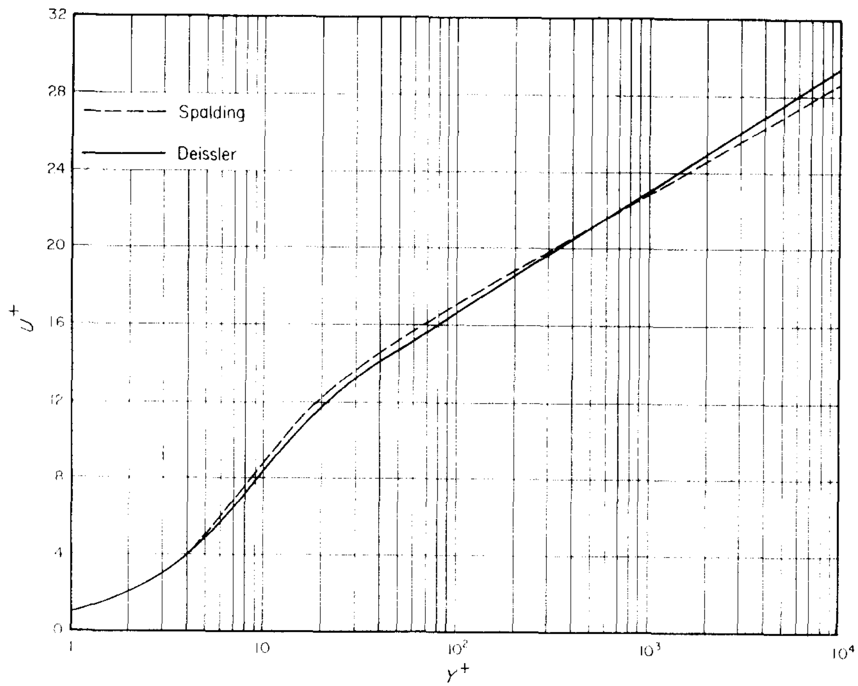

FIG. 1. The Deissler and Spalding forms of the "law of the wall".

$y^+ > 26 \quad u^+ =$

$$\frac{1}{0 \cdot 36} \ln \left(\frac{y^+}{26}\right) + 12 \cdot 8426 \qquad (9)$$

Figure 1 shows this relationship diagrammatically.

Since the expressions cover different ranges, the integration necessary must be carried out in two stages. We shall restrict the solution to values of Reynolds number where $y_s^+ > 26$ but we shall assume that the law is obeyed from the leading edge position. This cannot be true, of course, since there is an initial laminar zone but the previous analyses of this type have shown this assumption to give good results.

We first consider $\int_0^{y^+} (u^+)^2 \, dy^+$ needed in equations (4) and (5).

$$\int_0^{y^+} (u^+)^2 \, dy^+ = \int_0^{26} (u^+)^2 \, dy^+ + \int_{26}^{y^+} (u^+)^2 \, dy^+$$

Using equation (8) the value of $\int_0^{26} (u^+)^2 \, dy^+$ obtained by Runge–Kutta integration is 2250·47. (This calculation and all subsequent were performed on the Manchester University Atlas Computer.) The remainder of the integral can be performed analytically to yield

$$\int_0^{y^+} (u^+)^2 \, dy^+ = 7 \cdot 71606 \, y^+ (\ln y^+)^2 + 5 \cdot 63636 \, y^+ \ln y^+ + 8 \cdot 74536 \, y^+ - 583 \cdot 962 \qquad (10)$$

We may now determine a $R - y_s^+$ relation using (7).

Rewriting (7) as

$$R_2 - R_1 = \int_{y_{s1}^+}^{y_{s2}^+} \left[\int_0^{y_s^+} (u^+)^2 \, dy^+ \right] \frac{du_s^+}{dy_s^+} \, . \, dy_s^+$$

For values of $y_s^+ > 26$, (du_s^+/dy_s^+) is simply obtained as $(1/0 \cdot 36 y_s^+)$ from (9) and we obtain

$$R_y - R_{y_s^+ = 26} = 21 \cdot 4335 \, y_s^+ (\ln y_s^+)^2 - 27 \cdot 2105 \, y_s^+ (\ln y_s^+) - 1622 \cdot 13 \ln y_s^+ + 51 \cdot 5032 \, y_s^+ + 335 \cdot 426$$

$R_{y_s^+ = 26}$ is the Reynolds number corresponding to $y_s^+ = 26$ and if the profile is assumed to apply from the leading edge this can be computed using equation (8)

$$R_{26} = \int_0^{u_{26}^+} \left[\int_0^{26} (u^+)^2 \, dy^+ \right] du_s^+$$

The value of this integral was computed to be 4759·44. Hence we obtain

$$R_{y_s^+} = 21{\cdot}4335\, y_s^+ (\ln y_s^+)^2 - 27{\cdot}2105\, y_s^+ \ln y_s^+ - 1622{\cdot}13 \ln y_s^+ + 51{\cdot}5032\, y_s^+ + 5094{\cdot}86 \tag{11}$$

The shear stress variation is obtained by substituting equation (10) into equation (5) and the eddy diffusivity variation then follows from

$$\frac{\epsilon_m}{\nu y_s^+} = \left[0{\cdot}36 \frac{y^+}{y_s^+} \frac{\tau}{\tau_w} - \frac{1}{y_s^+}\right] \tag{12}$$

(b) *Spalding's law*

Spalding gives a form of the law of the wall which is a single equation and it is therefore more convenient for computation. It has the following form

$$y^+ = u^+ + 0{\cdot}1108 \left\{ \exp(0{\cdot}4\, u^+) - 1 - 0{\cdot}4\, u^+ - \frac{(0{\cdot}4\, u^+)^2}{2!} - \frac{(0{\cdot}4\, u^+)^3}{3!} - \frac{(0{\cdot}4\, u^+)^4}{4!} \right\} \tag{13}$$

Figure 1 shows this expression for comparison with Deissler's form. By similar arguments to the above we obtain

and from the above with (5) and (6) the shear stress and eddy diffusivity variations may be computed.

Polynomial fitting to $R - y_s^+$ and $R - u_s^+$ relations

As will be seen, in solving the energy equation it is necessary to have explicit relation for y_s^+ in terms of R in the case of Deissler's form and u_s^+ in terms of R in the case of Spalding's form.

Sixth degree polynomial equations were fitted to equations (11) and (14) in the following forms.

(a) *Deissler's profile*

$$\ln y_s^+ = a_1 z^6 + a_2 z^5 + a_3 z^4 + a_4 z^3 + a_5 z^2 + a_6 z + a_7 \tag{15}$$

(b) *Spalding's profile*

$$\ln u_s^+ = a_1 z^6 + a_2 z^5 + a_3 z^4 + a_4 z^3 + a_5 z^2 + a_6 z + a_7 \tag{16}$$

where $Z = \ln . R$ in each case.

Table 1 gives the values of the constants a_1 to a_7. By re-calculating these relations at known points the accuracy was found to lie between −0·032 and 0·0175 per cent for (15) and between −0·014 and 0·017 per cent for (16).

$R - x^+$ relations

Spalding [6] also introduced a new variable x^+ and in his analysis showed that solutions to the energy equation may be obtained using this

$$\int_0^{u^+} (u^+)^2 \, dy^+ = \frac{(u^+)^3}{3} + 0{\cdot}4 \times 0{\cdot}1108 \left\{ \frac{(u^+)^2 \exp(0{\cdot}4\, u^+)}{0{\cdot}4} - \frac{2}{(0{\cdot}4)^2} u^+ \exp(0{\cdot}4\, u^+) + \frac{2}{(0{\cdot}4)^3} \exp(0{\cdot}4\, u^+) - \frac{(u^+)^3}{3} - \frac{0{\cdot}4\,(u^+)^4}{4} - \frac{(0{\cdot}4)^2 (u^+)^5}{10} - \frac{(0{\cdot}4)^3 (u^+)^6}{36} - \frac{2}{(0{\cdot}4)^3} \right\}$$

$$\frac{dy^+}{du^+} = 1 + 0{\cdot}4 \times 0{\cdot}1108 \left\{ \exp(0{\cdot}4\, u^+) - 1 - 0{\cdot}4\, u^+ - \frac{(0{\cdot}4\, u^+)^2}{2!} - \frac{(0{\cdot}4\, u^+)^3}{3!} \right\}$$

$$R_{u_s^+} = \frac{(u_s^+)^4}{12} + 0{\cdot}4 \times 0{\cdot}1108 \left\{ \frac{(u_s^+)^2 \exp 0{\cdot}4\, u_s^+}{(0{\cdot}4)^2} - \frac{4}{(0{\cdot}4)^3} u_s^+ \exp(0{\cdot}4\, u_s^+) + \frac{6}{(0{\cdot}4)^4} \exp(0{\cdot}4\, u_s^+) - \frac{(u_s^+)^4}{12} - \frac{0{\cdot}4\,(u_s^+)^5}{20} - \frac{(0{\cdot}4)^2 (u_s^+)^6}{60} - \frac{(0{\cdot}4)^3 (u_s^+)^7}{252} - \frac{2u_s^+}{(0{\cdot}4)^3} - \frac{6}{(0{\cdot}4)^4} \right\} \tag{14}$$

Table 1. *Polynomial coefficients*

	Deissler's law	Spalding's law
a_1	$-2.3358264 \times 10^{-6}$	$-2.09921034 \times 10^{-7}$
a_2	$2.06615471 \times 10^{-4}$	2.049576×10^{-5}
a_3	$-7.52824874 \times 10^{-3}$	$-8.32415543 \times 10^{-4}$
a_4	0.143990399	$1.80627466 \times 10^{-2}$
a_5	-1.50727603	-0.223655719
a_6	8.78858606	1.60164079
a_7	-19.9065732	-2.45374632

variable in such a way that a universal curve is obtained, irrespective of the unheated starting length, when plotted against this parameter. His analysis however included the assumption that shear stress variations could be neglected and it would not be expected that his suggestion will apply when shear stress variation is included. However, for comparison purposes, the $R - x^+$ relation was calculated.

By definition

$$x^+ = \int_l^x \frac{\sqrt{(\tau_w)/\rho}}{\nu} \, dx$$

or

$$\frac{dx^+}{dR} = \frac{1}{u_s^+} \tag{17}$$

From the already determined $R - u_s^+$ relations it is possible to calculate x^+ for different values of the Reynolds number at which the discontinuity in temperature occurs for both Deissler's and Spalding's form.

Results of momentum solutions

Before proceeding further it may be helpful if the results obtained so far are discussed. Figures 2 and 3 show $R - u_s^+$ and $R - y_s^+$ [equations

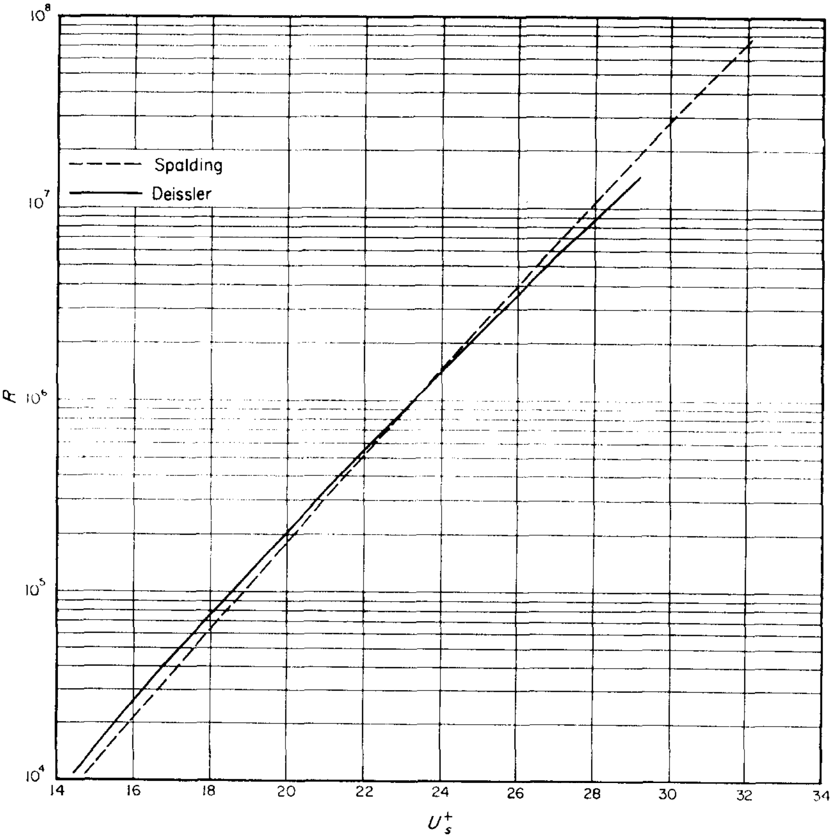

FIG. 2. Reynolds number—u_s^+ relations (Deissler's and Spalding's laws).

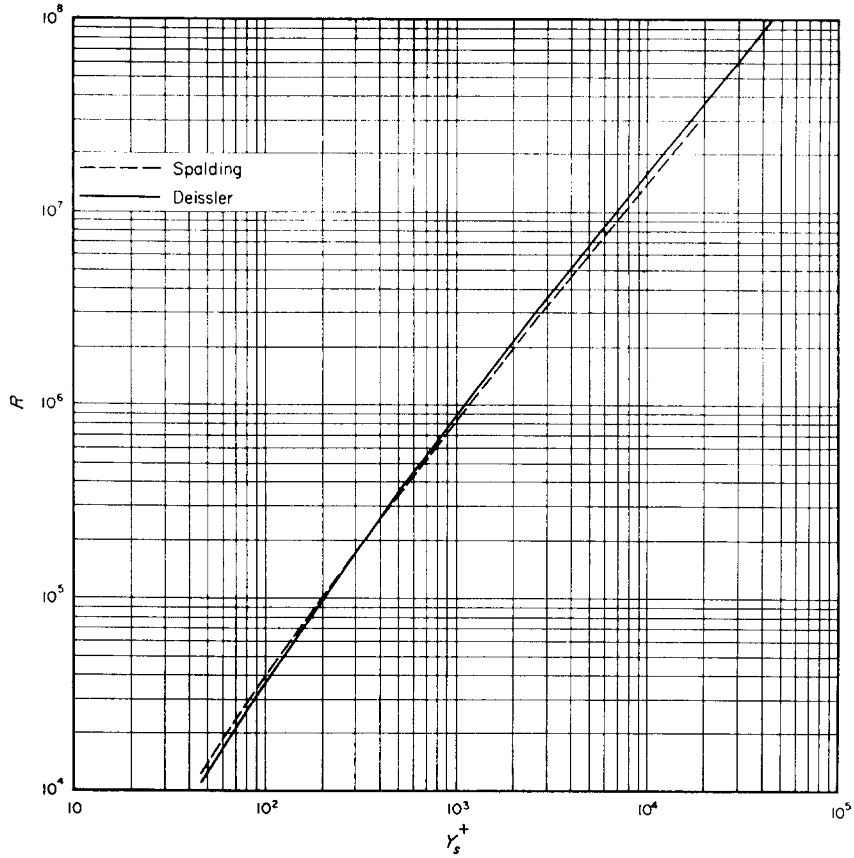

FIG. 3. Reynolds number—y_s^+ relations (Deissler's and Spalding's laws).

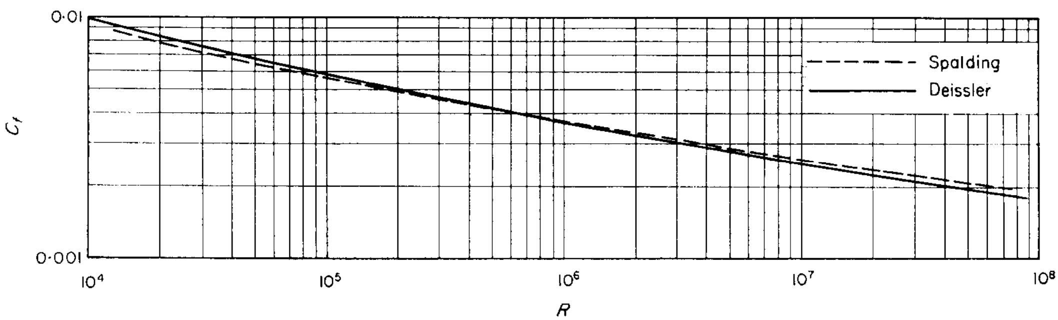

FIG. 4. Reynolds number—friction factor relations (Deissler's and Spalding's laws).

(11) and (14)] for both relationships. The polynomial approximations are used to generate these shapes in the energy solution. It is easily shown that

$$C_f = 2/(u_s^+)^2$$

and Fig. 4 shows the resulting variation of C_f with R. The Prandtl–Schlichting relation agrees very closely, tending towards the Deissler curve for R 10^4 to 10^6 and to the Spalding curve for R 10^6.

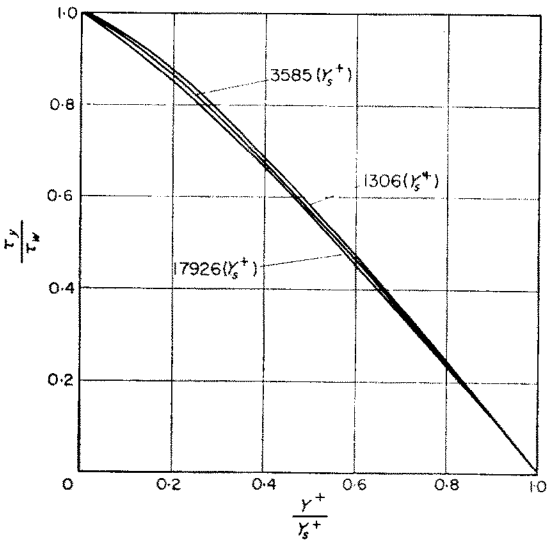

FIG. 5. Shear stress variation (Deissler's law).

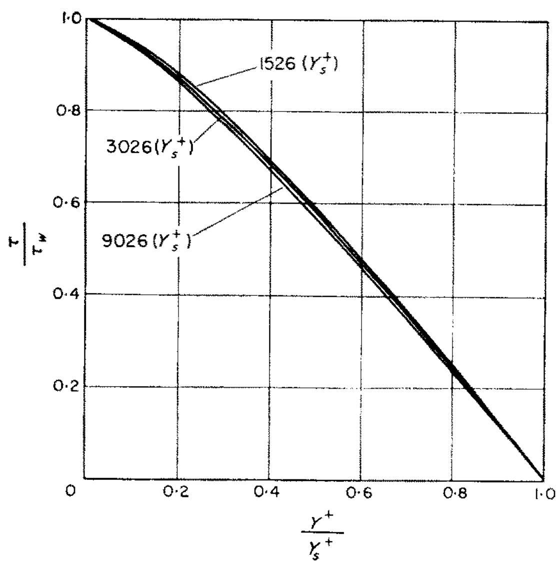

FIG. 6. Shear stress variation (Spalding's law).

Figures 5 and 6 show shear stress variations derived from equation (5) and the difference between the two forms of the law of the wall is extremely small. Figures 7 and 8 show the corresponding eddy diffusivity variation from equation (6). These curves are the main object of the momentum solution since they enable us to proceed to the energy equation solution if the assumption $\epsilon_h = \epsilon_m$ is made. There is little variation in these curves with R but in the energy solution the exact equations were used. It is worth noting that the maximum ϵ_m is some 12 per cent higher for Spalding's form than for Deissler's form. Finally Fig. 9 shows the variation of x^+ with R and for both cases the curves are indistinguishable.

Energy equation solution

The basic energy equation for a turbulent incompressible boundary layer is written as

$$u\frac{\partial \theta}{\partial x} + v\frac{\partial \theta}{\partial y} = \frac{\partial}{\partial y}\left\{(\alpha + \epsilon_h)\frac{\partial \theta}{\partial y}\right\}. \qquad (18)$$

By using the same transformation as before we may arrive at

$$u^+ u_s^+ \frac{\partial \theta}{\partial R} = \frac{\partial}{\partial y^+}\left\{\left(\frac{1}{Pr} + \frac{\epsilon_h}{\nu}\right)\frac{\partial \theta}{\partial y^+}\right\} \qquad (19)$$

and the solution to this equation is the main object of the work. The boundary conditions on this equation are

$$\theta = 1 \quad \text{all } y^+ \qquad x < l$$
$$\theta = 0 \quad \text{at } y^+ = 0 \qquad x > l$$

The solution was carried out by a finite difference method similar to the well-known Schmidt method. In order to provide for the steep slope of the $u^+ - y^+$ relation near the wall it is necessary to use very small steps of Δy^+ which implies very small steps of ΔR. In order to speed up the calculation to achieve useful results over a wide range of R, it was carried out in two parts in the following manner:

(1) For the region close to the temperature discontinuity, steps of $\Delta y^+ = 2$ were used. This was carried on for a moderately small increase of R and then discontinued.

(2) A simplifying assumption was made, namely, that the heat capacities of the layers up to $y^+ = 26$ for Deissler's form and up to $y^+ = 10$ for Spalding's form are negligible, i.e. in these thin layers a "steady-state" solution was used. This permitted much larger steps in Δy^+ and hence in ΔR.

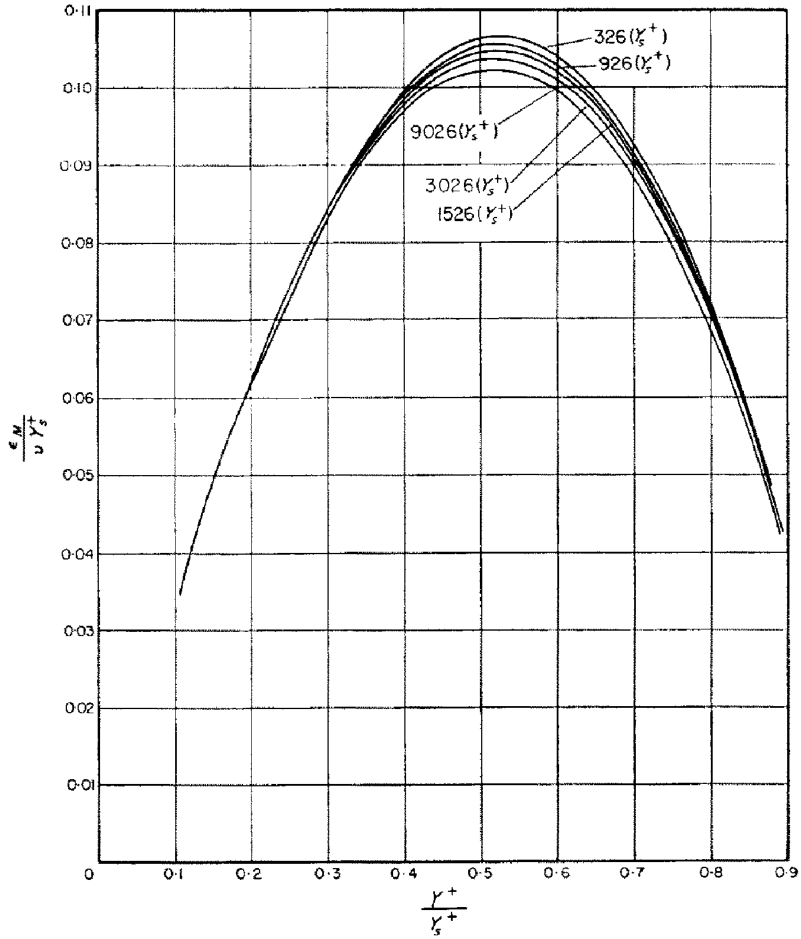

FIG. 7. Eddy diffusivity for momentum variation (Deissler's law).

In these parts this assumption implies

$$\frac{\partial}{\partial y^+}\left\{\beta \frac{\partial \theta}{\partial y^+}\right\} = 0$$

Hence

$$\theta = C\int_0^{y^+} \frac{1}{\beta} \mathrm{d}y^+ + K$$

where $y^+ = 26$ or 10 according to the law of the wall.

Now $\theta = 0$ when $y^+ = 0$ thus $K = 0$ and

$$C = \frac{\theta_{y^+=26}}{\int_0^{26} (1/\beta)\, \mathrm{d}y^+} \quad \text{(Deissler's form)}$$

The value of C along the layer $y^+ = 26$ varies with R. Its initial value may be found at the position of the jump step since at this point $\theta = 1$ at $y^+ = 26$.

Thus

$$C_i = \frac{1}{\int_0^{26} (1/\beta)\, \mathrm{d}y^+} \tag{20}$$

The value of C can now be calculated for subsequent steps in ΔR from

$$C = \theta_{y^+=26} \,.\, C_i \tag{21}$$

The values of C_i are given in Table 2.

The two solutions were observed to merge after a short increment in R and this was assumed to justify the assumption (2).

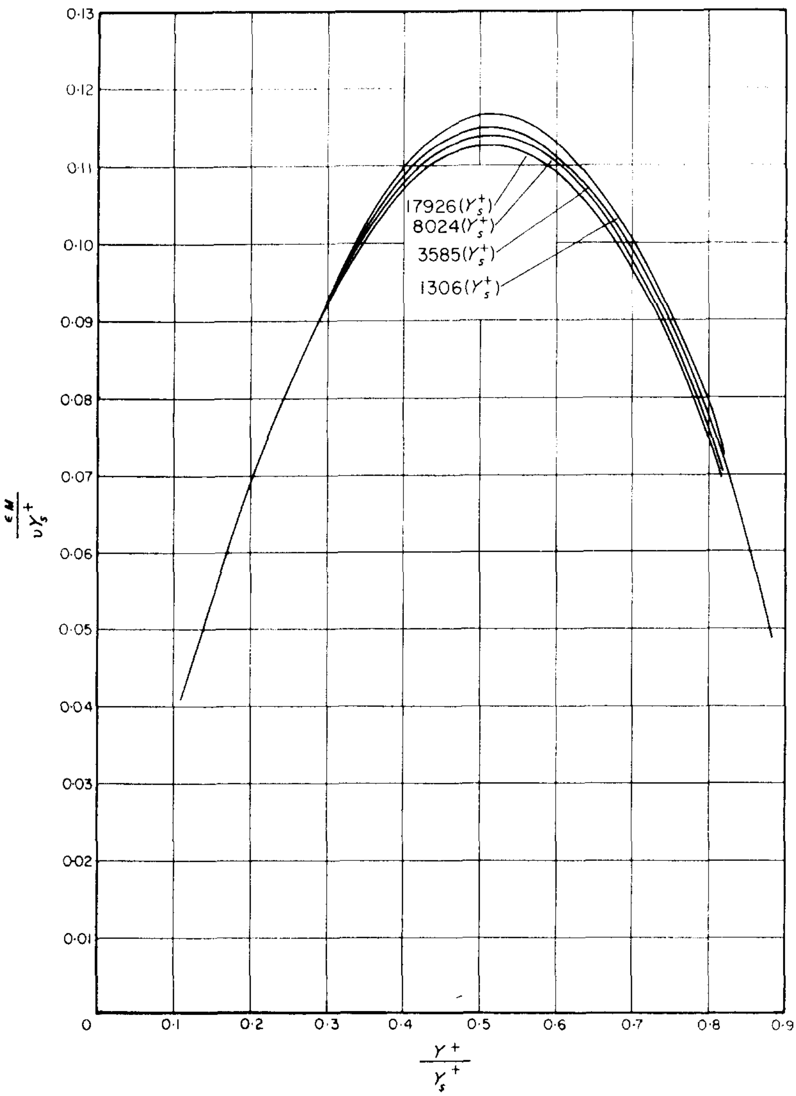

FIG. 8. Eddy diffusivity for momentum variation (Spalding's law).

Table 2. Values of C_i required for energy equation solution assuming a steady-state solution near the wall

	C_i	
Pr	Deissler†	Spalding‡
0·01	3·91940	10·01543
0·10	0·450507	1·0188165
0·70	0·099380	0·1560326
1·00	0·077860	0·11246108
10·00	0·016886	0·01589504

† Steady-state solution up to $y^+ = 26$.
‡ Steady-state solution up to $y^+ = 10$.

Finite difference scheme

When converted into finite difference form equation (19) becomes

$$\theta_i^* = \theta_i \left[1 - \frac{2 \,.\, \Delta R \,.\, \beta_i}{u_i^+ \; u_s^+ \; (\Delta y^+)^2}\right] + \theta_{(i+1)} \left[\frac{\Delta R}{u_i^+ \; u_s^+ \; (\Delta y^+)^2} \left\{\beta_i + \beta_i' \frac{\Delta y^+}{2}\right\}\right] + \theta_{(i-1)} \left[\frac{\Delta R}{u_i^+ \; u_s^+ \; (\Delta y^+)^2} \left\{\beta_i + \beta_i' \frac{\Delta y^+}{2}\right\}\right] \quad (22)$$

See Fig. 10(a).

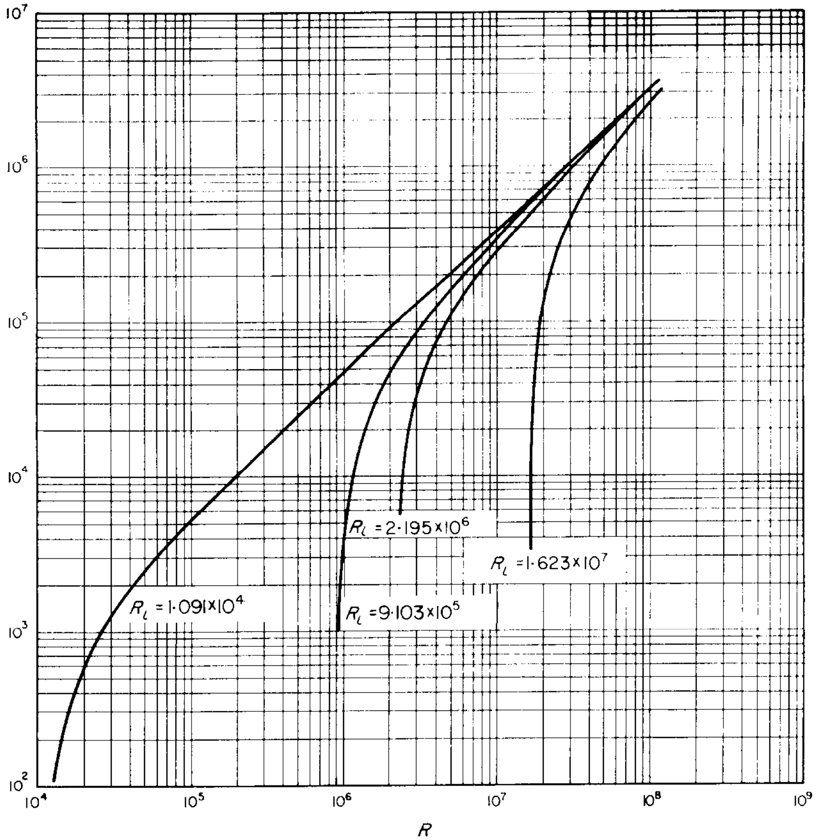

FIG. 9. Reynolds number—x^+ variation (Deissler's and Spalding's laws).

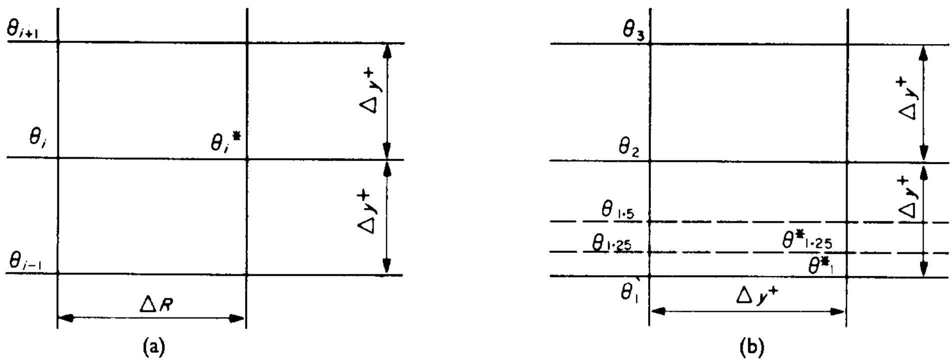

FIG. 10. Finite difference meshes.

For assumption (1) this applies to all points including the surface ($i = 1$). For assumption (2) the solution is taken out from the layer $y^+ = 26$ (Deissler) or $y^+ = 10$ (Spalding) and these were chosen as the $i = 1$ position. However, in these cases a special treatment of the surface is necessary since θ_1 is not constant with R at these positions.

Making the assumption $\theta^*_{1\cdot 25} - \theta_{1\cdot 25} \doteqdot \theta^*_1 - \theta_1$ the energy equation becomes

$$\theta_1^* = \theta_1 \left[1 - \frac{2 \, . \, \Delta R \, . \, \beta_{1.5}}{u_{1\cdot25}^+ \; u_s^+ \; (\Delta y^+)^2}\right] + \theta_2 \, . \, \frac{2 \, . \, \Delta R \, . \, \beta_{1.5}}{u_{1\cdot25}^+ \, u_s^+ \, (\Delta y^+)^2} - \frac{2C \, . \, \Delta R}{u_{1\cdot25}^+ \, u_s^+ \; \Delta y^+} \tag{23}$$

See Fig. 10(b).

Whether assumption (2) was made or not the stability limit occurred in the region of maximum β, so that the step length ΔR must be limited by

$$\frac{2 \Delta R \, . \, \beta_i}{u_i^+ \; u_s^+ \; (\Delta y^+)^2} < 1 \tag{24}$$

The programme was arranged to determine the maximum value of this parameter for every step and it adjusted the next step ΔR accordingly with some safety margin. Figure 11 shows the maximum values of $(\beta_i/u_i^+ u_s^+)$ (the important part of the stability number) plotted against y_s^+ and it will be seen that low Prandtl numbers impose a more severe stability criterion on the numerical process.

The Stanton number is easily shown to be

$$St = \frac{1}{Pr \, . \, u_s^+} \left(\frac{\partial \theta}{\partial y^+}\right)_{y^+ = 0}$$

The slope at the wall was obtained from a five point differentiation formula when assumption (1) was used.

When assumption (2) was used $(\partial\theta/\partial y^+)_{y^+=0}$ becomes $C \, . \, Pr$ thus $St = C/u_s^+$ in this case. The Spalding number $(\partial\theta/\partial y^+)_{y^+=0}$ may also be obtained.

RESULTS AND CONCLUSIONS

The solution was obtained for five Prandtl numbers (0·01, 0·1, 0·7, 1 and 10) and for four positions of the jump step (at $y_s^+ = 46$, 1026, 2026, 10026). These positions were chosen arbitrarily but it was slightly simpler to choose these rather than R for Deissler's profile. However, the corresponding values of R were chosen for the Spalding profile to make the results comparable (these are $1{\cdot}091 \times 10^4$, $9{\cdot}103 \times 10^5$, $2{\cdot}195 \times 10^6$, $1{\cdot}623 \times 10^7$).

The results in the form St versus R are shown in Figs. 12 and 13. The differences in St between the two profiles are quite small except in the region of high Reynolds number where the values given by Spalding's form lie higher than those given by Deissler's law (at $R = 10^8$ and for $Pr \leqslant 0{\cdot}7$ the difference is of the order of 25 per cent). Nevertheless the reasonably close

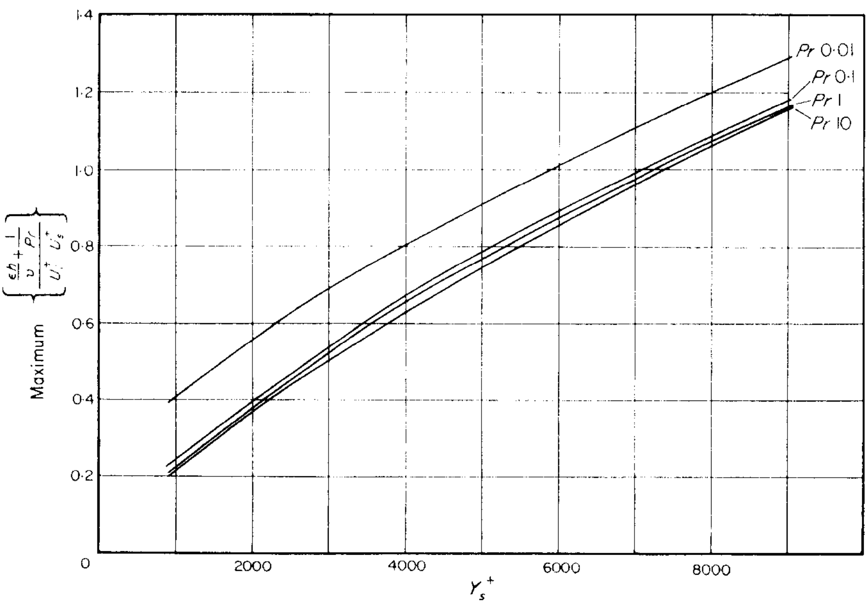

FIG. 11. Variation of the maximum stability parameter with y_s^+ and Prandtl number.

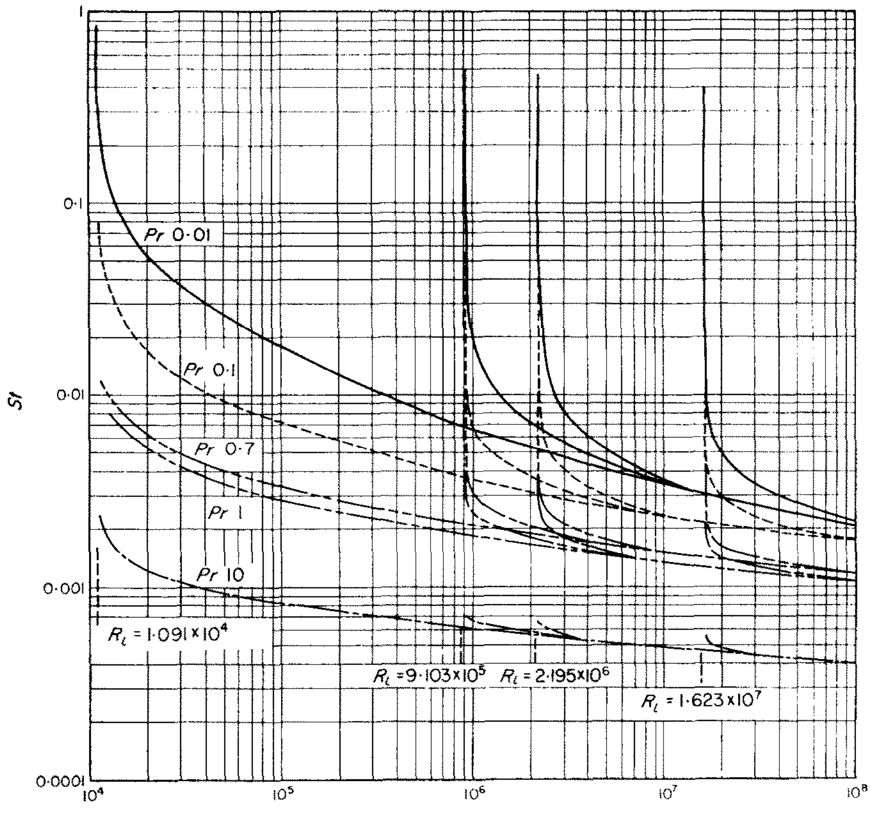

FIG. 12. Reynolds number—Stanton number variation for different positions of the jump step in temperature for Deissler's form of the law of the wall.

agreement gives confidence in the accuracy of the numerical procedures.

The influence of the different starting position is clearly shown, the Stanton number falling eventually on to a common curve. For high Prandtl numbers this convergence is very rapid. A number of suggested empirical correlations (see for example [5]) were tried in an attempt to bring these results on to a single curve for all Prandtl numbers but none was satisfactory.

The assumption that $\epsilon_h/\epsilon_m = 1$ has been shown recently to be incorrect for flow in pipes and, although there exists no data on this ratio in turbulent boundary layers, similar effects are no doubt present. For this reason the results of Figs. 12 and 13 must be considered doubtful, particularly at low Prandtl numbers. If reliable data on the eddy diffusivity ratio becomes available it would be straightforward to include it in the general method.

Figure 14 shows the results in the form of $Sp - x^+$. The important feature here is that for $Pr \geqslant 0{\cdot}7$ the curves for different starting lengths are indistinguishable showing that the influence of including the variation of shear stress is negligible. For Prandtl number 0·1 and 0·01 however the effect becomes noticeable and a single curve does not correlate the effect of different starting lengths.

Table 3 gives some numerical values of the Spalding number, together with those calculated by Kestin and Gardner [10] and Smith and Shah [9] and it will be seen that these compare closely. The present values were interpolated to only four significant figures since the inclusion of the shear stress variation causes differences

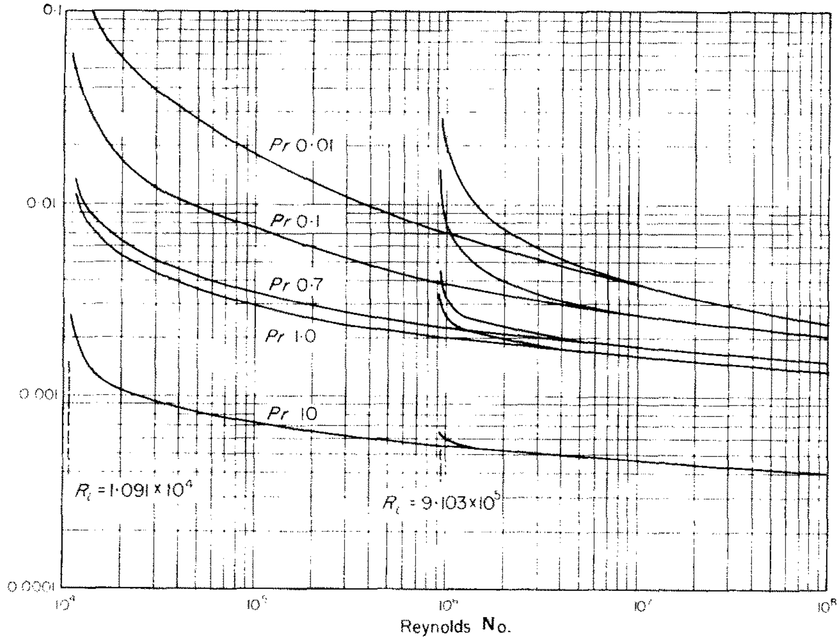

FIG. 13. Reynolds number—Stanton number variation for different positions of the jump step in temperature for Spalding's form of the law of the wall.

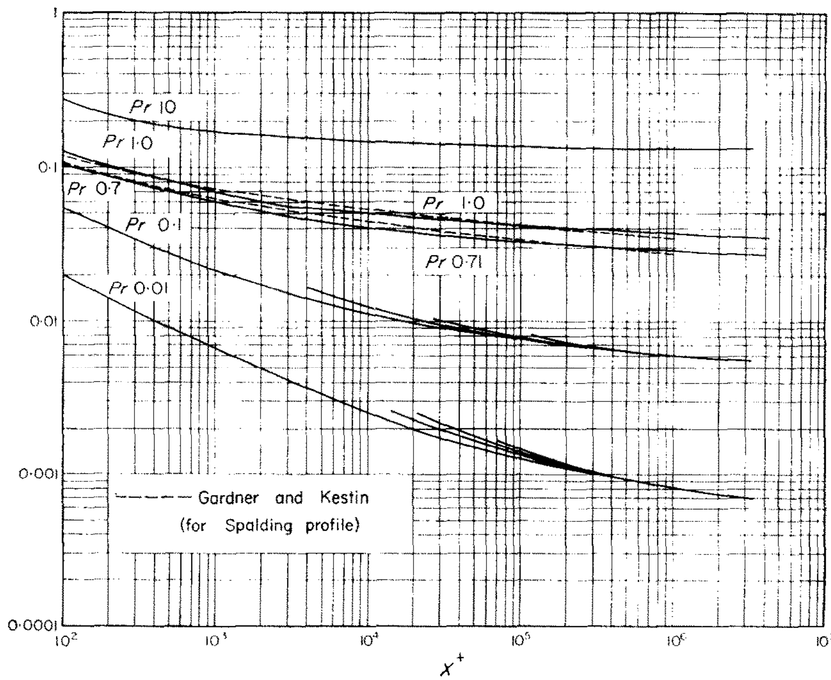

FIG. 14. Variation of Spalding's function with x^+ (showing that the different starting positions do not correlate onto a single curve at low Prandtl number).

Table 3. *Values of the Spalding function obtained in this analysis by other authors*

x^+	Present analysis (Deissler's law)	Gardner† and Kestin (Spalding's law)	Smith and Shah (Spalding's law)
For *Pr* 0·7			
10^2	0·1040	0·10720	0·125829
10^3	0·0600	0·06248	0·0680106
10^4	0·0405	0·04428	0·045754
10^5	0·0330	0·03407	0·034666
10^6	0·0290	0·02731	0·027762
For *Pr* 1			
10^2	0·1250	0·1200	0·14177
10^3	0·0700	0·07151	0·07728
10^4	0·0505	0·05288	0·054413
10^5	0·0420	0·04205	0·042931
10^6	0·0373	0·03456	0·035321

† Gardner and Kestin's results are for *Pr* 0·71 and 1.

in the x^+ values with different starting lengths if the numbers are calculated to higher precision.

In general one may conclude that for Prandtl numbers greater than 0·7 the results of this calculation confirm those of previous workers. For values less than 0·7 where no previous information is available, it would be easily possible by cross-plotting from Fig. 12 to obtain good estimations of the variation of Stanton number in a turbulent boundary layer on a flat plate with a step change of surface temperature at any position.

ACKNOWLEDGEMENT

The author would like to express his gratitude to his research students A. H. Sugden and S. Subramanyan who carried out much of the detailed programming of the calculations described in this work and to Professor D. B. Spalding for some useful conversations.

REFERENCES

1. M. W. Rubesin, Effect of an arbitrary surface temperature variation along a flat plate on the convective heat transfer in an incompressible turbulent boundary layer, *NACA TN* 2345 (1951).
2. S. Scesa and F. M. Sauer, An experimental investigation of convective heat transfer to air from a flat plate with a stepwise discontinuous surface temperature, *Trans. Amer. Soc. Mech. Engrs* **74**, 1251 (1952).
3. P. R. Owen and A. O. Ormerod, Evaporation from the surface of a body in an air stream, *R.A.E.* Aero 2431, *R & M* No. 2875 (1951).
4. B. N. Furber, Some heat and mass transfer experiments on humid air in turbulent flow over a flame containing an isolated cooled region. Ph.D. Thesis, University of Manchester (1953).
5. W. C. Reynolds, W. M. Kays and S. J. Kline, A summary of experiments on turbulent heat transfer from a non isothermal plate, *Trans. Amer. Soc. Mech. Engrs, J. Heat Transfer* **82**, 341 (1960).
6. D. B. Spalding, Heat transfer to a turbulent stream from a surface with a stepwise discontinuity in wall temperature. *Int. Developments in Heat Transfer*, Part II, p. 439. ASME (1961).
7. D. B. Spalding, A single formula for the law of the wall, *Trans. Amer. Soc. Mech. Engrs, J. Appl. Mech.* **81**, Ser. E, 455 (1961).
8. J. Kestin and L. N. Persen, Application of Schmidt's method to the calculation of Spalding's function and of the skin friction coefficient in turbulent flow, *Int. J. Heat Mass Transfer* **5**, 143 (1962).
9. A. G. Smith and V. L. Shah, The calculation of wall and fluid temperatures for the incompressible turbulent boundary layer, with arbitrary distribution of wall heat flux, *Int. J. Heat Mass Transfer* **5**, 1179 (1962).
10. G. O. Gardner and J. Kestin, Calculation of the Spalding function over a range of Prandtl numbers, *Int. J. Heat Mass Transfer* **6**, 289 (1963).
11. J. Kestin and P. D. Richardson, Heat transfer across turbulent incompressible boundary layers, *Int. J. Heat Mass Transfer* **6**, 147 (1963).
12. R. G. Deissler, Analysis of turbulent heat transfer, mass transfer and friction in smooth tubes at high Prandtl and Schmidt numbers, *NACA TN* 3145 (1954); also Report 1210 (1955).

Résumé—A partir de l'hypothèse que le profil de vitesse sans dimensions dans une couche limite turbulente incompressible obéit au profil universel bien connu, on montre que l'épaisseur de la couche limite et les variations de la contrainte de cisaillement et de la diffusivité turbulente à travers l'épaisseur peuvent être obtenues à n'importe quel nombre de Reynolds. On montre que les variations résultantes, exprimées sous forme non dimensionnelle, dépendent seulement et faiblement du nombre de Reynolds.

En utilisant l'hypothèse supplémentaire que les diffusivités turbulentes pour la quantité de mouvement et la chaleur sont égales, l'équation de l'énergie est résolue numériquement pour obtenir la variation du nombre de Stanton avec le nombre de Reynolds pour plusieurs nombres de Prandtl de 0,01; 0,7; 1,0 et 10 et pour différentes positions d'une distribution de température par échelon sur la plaque plane.

Zusammenfassung—Mit der Annahme, dass das dimensionslose Geschwindigkeitsprofil in einer turbulenten inkompressiblen Grenzschicht dem bekannten Universalprofil entspricht, können Grenzschichtdicke, Schubspannung und Änderungen der Austauschfaktoren in der Grenzschicht bei beliebigen Reynolds-Zahlen ermittelt werden. Die resultierenden, in dimensionsloser Form wiedergegebenen Änderungen zeigen sich nur sehr wenig abhängig von der Reynolds-Zahl.

Mit der weiteren Annahme, dass die Austauschfaktoren für Impuls und Energie gleich sind, wird die Energiegleichung numerisch gelöst, um die Änderung der Stanton-Zahl mit der Reynolds-Zahl für verschiedene Prandtl-Zahlen zu erhalten. Ergebnisse sind für die Prandtl-Zahlen 0,01, 0,1, 0,7, 1,0 und 10 und für verschiedene Anordnungen einer sprunghaften Temperaturverteilung an einer ebenen Platte angegeben.

Аннотация—Показано, что исходя из допущения о том, что безразмерный профиль скорости в турбулентном несжимаемом пограничном слое подчиняется известному универсальному профилю, можно определить толщину пограничного слоя и изменение напряжения трения и коэффициента турбулентной диффузии через пограничный слой для любого числа Рейнольдса. Получающиеся в результате изменения, выраженные в безразмерной форме, незначительно зависят от числа Рейнольдса.

Используя дополнительные допущения, что коэффициенты турбулентной диффузии для количества движения и теплоты равны, можно численно решить уравнение энергии, чтобы получить зависимость числа Стантона. от числа Рейнольдса для нескольких чисел Прандтля. Приводятся результаты для чисел Прандтля 0,01, 0,1, 0,7, 1,0 и 10, для различных положений ступенчатого распределения температуры на плоской пластине.